

Supporting Information

© Wiley-VCH 2011

69451 Weinheim, Germany

Improved Stability and Smart-Material Functionality Realized in an Energetic Cocrystal**

*Onas Bolton and Adam J. Matzger**

ange_201104164_sm_miscellaneous_information.pdf

Supporting Information

Table of Contents

- SI 1. Experimental
- SI 2. Optical Microscopy
- SI 3. Raman Spectroscopy
- SI 4. Powder X-ray Diffraction
- SI 5. Single Crystal X-ray Diffraction
- SI 6. Differential Scanning Calorimetry (DSC)
- SI 7. References

SI 1. Experimental

Caution: Although no unplanned detonation was encountered during this work, CL-20 and TNT are both dangerous high explosives. Proper safety practices and equipment must be used to prevent explosion due to friction, heat, static shock, or impact. Be aware that the potential for severe injury exists if these materials are improperly handled.

2,4,6,8,10,12-Hexanitro-2,4,6,8,10,12-hexaazaisowurtzitane (CL-20) was received from the China Lake Naval Air Weapons Station. 2,4-Dinitrotoluene was purchased from Acros Organics. 2,4,6-Trinitrotoluene (TNT) was synthesized by treating 2,4-dinitrotoluene with fuming nitric acid.

Crystallization

A glass vial was loaded with 4.38 mg of CL-20 (10 μmol) and 2.27 mg of TNT (10 μmol) then dissolved into 1 mL of ethanol. Sonication and mild heating was used to dissolve all CL-20. The solvent is allowed to evaporate at 23 $^{\circ}\text{C}$ over several days. Colorless prisms of 1:1 CL-20:TNT cocrystal (**1**) were formed. Alternative solvents reliably producing this cocrystal form include acetonitrile, ethyl acetate, tetrahydrofuran, acetone, 1,4-dioxane, methanol, and 1-propanol.

Solvent-mediated cocrystallization was conducted by charging a vial with 166.1 mg of β -CL-20 (0.38 mmol), 86.1 mg of TNT (0.38 mmol), and a single seed crystal of **1**, approximately 0.2 mg, prepared as described above. One mL of 2-propanol is added to the vial. The slurry is shaken on an IKA model KS 260 shaker for three days, in which time all solids were converted to **1**.

SI 2. Optical Microscopy

Images of **1** prisms were collected using a Spot Advanced camera through a Leica microscope coupled with a 10x objective. Images were processed using Spot Advanced software.

SI 3. Raman Spectroscopy

Raman spectra were collected using a Renishaw inVia Raman microscope equipped with a Leica microscope, RenCam CCD detector, 647 nm laser, 1800 lines/nm grating, and 50 μm slit. Spectra were collected in extended scan mode in the range of 3600-100 cm^{-1} and then analyzed using the Wire 3.1 software package. Calibration was performed using a silicon standard.

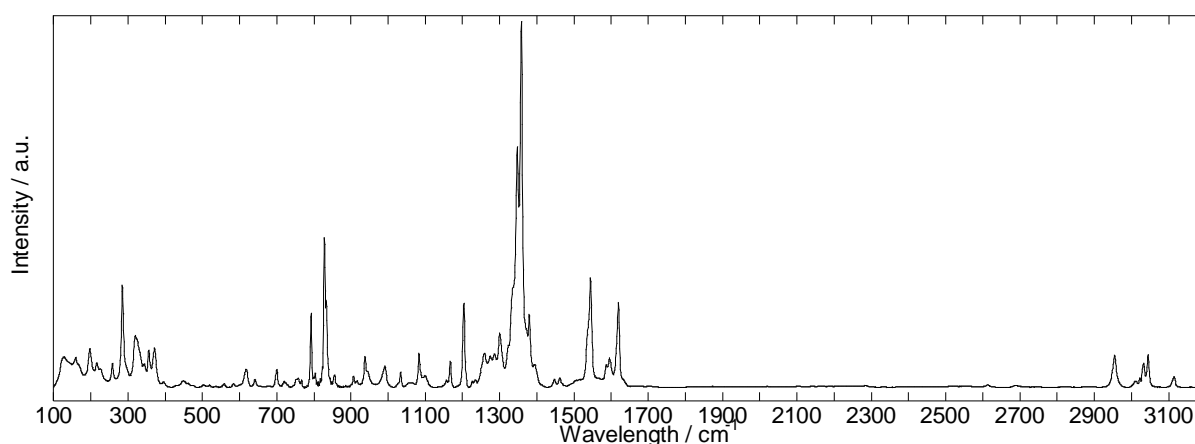


Figure S1. Enlarged Raman Spectrum of **1**.

Table S1. Frequency of Raman vibrational modes (cm^{-1}) in **1**.

157.9	828.4	1358.0
196.4	937.7	1379.5
216.4	990.0	1544.3
257.9	1083.2	1596.6
284.9	1167.1	1618.9
318.8	1204.0	2954.5
331.1	1259.4	3023.0
355.7	1285.6	3033.0
371.1	1300.2	3044.6
618.2	1334.9	3113.9
792.9	1348.0	

SI 4. Powder X-ray Diffraction

Powder X-ray diffraction (PXRD) patterns were collected at ambient temperature using a Bruker D8 Advance diffractometer operating at 40 kV and 40 mA with Cu-K α radiation (1.5406 Å). A sample of approximately 25 mg of **1**, prepared from slurry, was finely ground and placed on an indented glass slide. The spectrum was collected by scanning 2θ from 3° to 90° at with a step size of 0.015°. The step time was 2 s. Powder patterns were processed using Jade Plus^[1] to calculate peak positions and intensities.

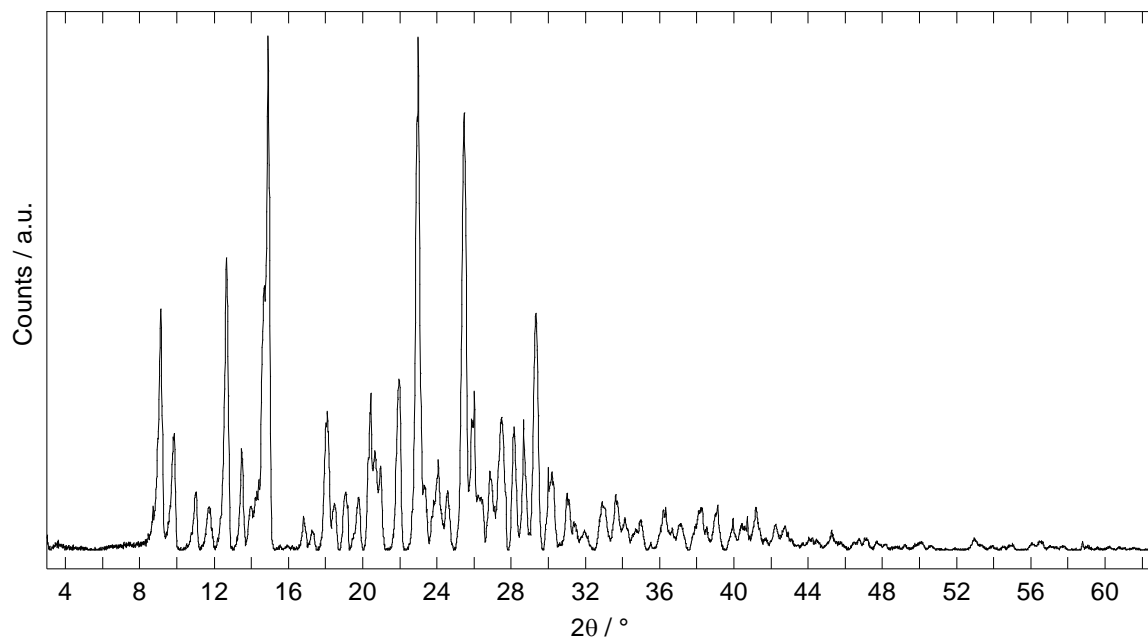


Figure S2. Enlarged PXRD Pattern of **1**.

Table S2. Experimental PXRD peak position and the relative intensity of **1**.

2θ (°)	I/I_0 (%)	FWHM (°)	2θ (°)	I/I_0 (%)	FWHM (°)
9.1	46.9	0.24	27.5	26	0.36
9.9	22.8	0.28	28.2	24	0.24
11.0	11.3	0.23	28.7	22.6	0.60
11.7	8.6	0.28	29.4	47	0.28
12.7	58.1	0.23	30.2	16.5	0.40
13.5	19.6	0.21	31.1	11.4	0.35
14.0	9.6	0.24	31.5	5.8	0.50
14.7	49.9	0.86	32.0	3.8	0.37
14.9	100	0.30	33.0	8.5	0.38
16.8	5.9	0.20	33.7	9.6	0.39
17.3	3.7	0.24	34.1	5.4	0.53
18.1	27.6	0.30	34.7	3.6	0.62
18.5	10	0.34	35.0	5.6	0.41
19.1	13.2	0.28	36.3	9.1	0.44
19.8	12.6	0.33	36.7	5	0.86
20.5	31.8	0.38	37.2	6.4	0.40
20.7	20.4	0.62	38.2	9	0.54
21.0	16.9	0.44	39.1	8.3	0.32
22.0	32.9	0.25	40.0	4.9	0.20
23.0	97.7	0.27	40.4	4.4	0.50
23.4	12.3	0.81	41.2	7.5	0.37
24.1	16.5	0.39	42.3	4.7	0.46
24.6	11	0.29	42.8	4.8	0.72
25.5	82.6	0.27	44.2	2.3	0.44
26.0	29.6	0.63	45.3	3.3	0.48
26.4	10	0.22	46.7	2.1	0.55
26.9	14.6	0.33	47.2	2.4	0.44

SI 5. Single Crystal X-ray Diffraction

All measurements were made on a Rigaku RAXIS Spider diffractometer with an imaging plate area detector using graphite monochromated Cu-K α radiation (1.5406 Å). The data collection was made at 95 K. The structure was solved by direct methods^[2] and expanded using Fourier techniques. The non-hydrogen atoms were refined anisotropically and the hydrogen atoms were refined using the riding model. The final cycle of full-matrix least-squares refinement was made on F². An empirical absorption correction was applied to the structure. All calculations were performed using the CrystalStructure^[3] crystallographic software package except for refinement, which utilized SHELXL-97.^[4]

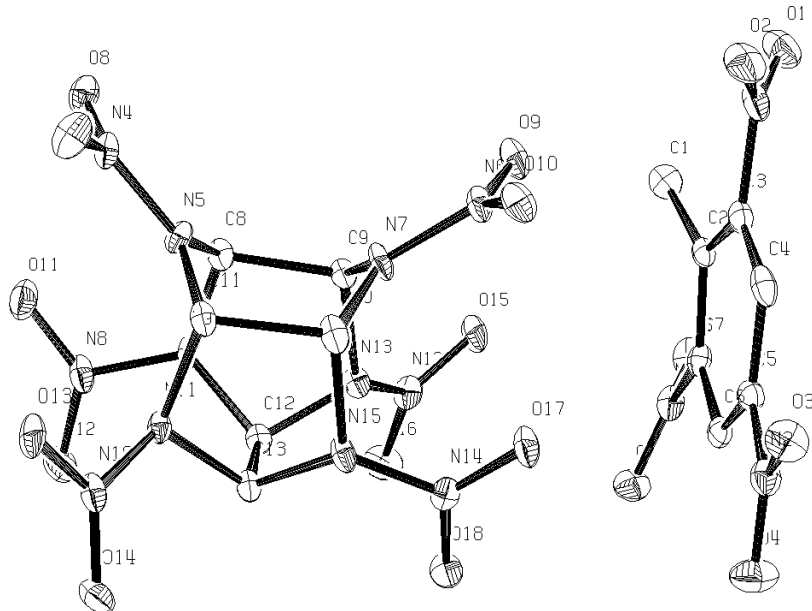


Figure S3. ORTEP diagram of **1** with 50% probability ellipsoids.

SI 6. Differential Scanning Calorimetry

Thermograms of the samples were recorded on a TA Instruments Q10 DSC. The thermal behavior of the samples, placed in sealed aluminum pans, was studied under nitrogen purge with a heating rate of 10 °C min⁻¹ covering the temperature range 50 °C to 300 °C. The instrument was calibrated with an indium standard. A notably lower decomposition temperature observed for CL-20 grown from thermal conversion of **1**, relative to that of pure CL-20, is believed to be due to the highly defective character of crystals grown in this way.

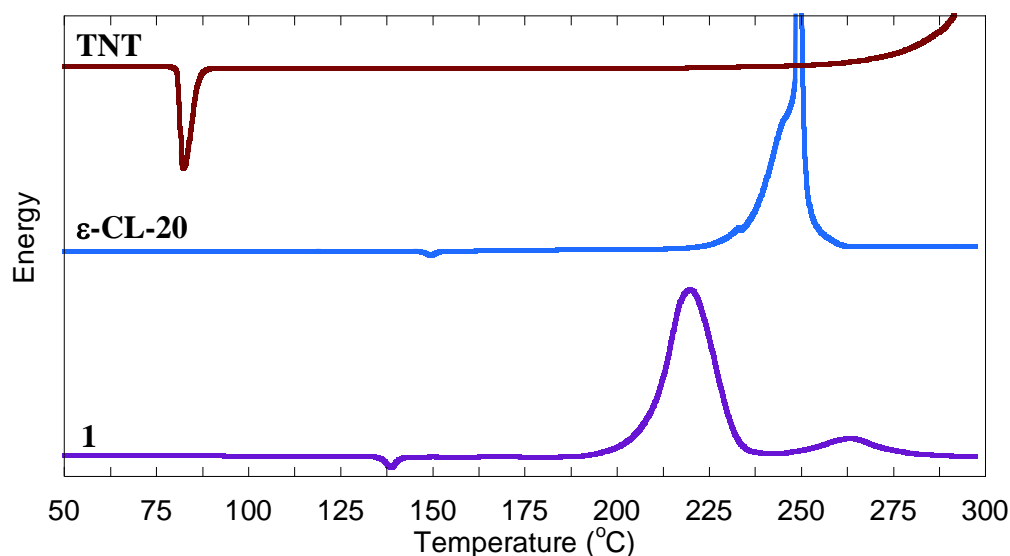


Figure S4. DSC traces of TNT (melting onset = 80 °C, decompositions onset = 283 °C), ϵ -CL-20 (conversion to γ -form onset = 145 °C, decomposition onset = 227 °C), and **1** (conversion to liquid TNT and β -CL-20 onset = 136 °C, decomposition of CL-20 onset = 205 °C, and decomposition of TNT onset = 247 °C). States were confirmed by halting the tests at various points and analyzing the sample with Raman spectroscopy.

SI 7. References

- [1] Jade Plus 8.2 ed.; Materials Data, Inc. 1995-2007.
- [2] M.C. Burla, R. Caliendo, M. Camalli, B. Carrozzini, G.L. Cascarano, L. De Caro, C. Giacovasso, G. Polidori, R. Spagna, *J. Appl. Crystallogr.* **2005**, *38*, 381.
- [3] CrystalStructure 4.0 ed.; Crystal Structure Analysis Package, Rigaku and Rigaku/MSK: The Woodlands, TX 77381, 2000-2009.
- [4] G.M. Sheldrick, (1997). SHELXS97 and SHELXL97. University of Göttingen, Germany.